European Journal of Control (2004)10:105–116

European Journal of Control

Global Stabilization of a Nonlinear Ginzburg–Landau Model of Vortex Shedding

Ole Morten Aamo[1] and Miroslav Krstić[2]

[1]Department of Engineering Cybernetics, Norwegian University of Science and Technology, N-7491 Trondheim, Norway; [2]Department of MAE, University of California at San Diego, La Jolla, CA 92093-0411, USA

We design a state feedback controller that achieves global asymptotic stabilization of a nonlinear Ginzburg–Landau model of vortex shedding from bluff bodies. Stabilization is obtained in two steps. First, the upstream and downstream parts of the system are shown to exhibit the ISS property with respect to certain boundary input terms governed by the core flow in the vicinity of the bluff body. Second, a finite difference approximation of arbitrary order of the core flow is stabilized using the backstepping method. Consequently, all the states in the core flow are driven to zero, including the boundary input terms of the upstream and downstream subsystems. The control design is valid for any Reynolds number. Numerical simulations are provided in order to demonstrate the performance of the controller, along with the potential of using low order discretizations for the control design, and thereby reducing the number of sensors needed for implementation.

Keywords: Partial Differential Equations; Flow Control; Feedback; Backstepping

1. Introduction

In flows past submerged obstacles, the phenomenon of vortex shedding occurs. For flow past a two-dimensional (2D) circular cylinder, which is a prototype model flow for studying vortex shedding, vortices are alternatively shed from the upper and lower sides of the cylinder, subjecting the cylinder to periodic forcing. In practice the periodic forcing leads to structural vibrations, which are associated with penalties ranging from passenger discomfort to structural damage or failure from fatigue. Consequently, suppression of vortex shedding is of great importance in many engineering applications. For a thorough review of the dynamics of the cylinder wake, see [14].

Naturally, the flow past a 2D circular cylinder has also been a popular model flow for studying vortex suppression by means of open-loop or feedback control. For Reynolds numbers slightly larger than the critical value for onset of vortex shedding (which is $\sim R_c = 47$), several authors have successfully suppressed vortex shedding in numerical simulations using various simple feedback control configurations. In [11], a pair of suction/blowing slots positioned on the cylinder wall were used for actuation, and shedding was suppressed for $R = 60$, using proportional feedback from a single velocity measurement taken some distance downstream of the cylinder. For $R = 80$, vortex shedding was reduced, but not completely suppressed. In [7], the same actuation configuration was tried using feedback from a pair of pressure sensors located on the cylinder wall for $R = 60$. This attempt was unsuccessful, but by adding

Correspondence to: O.M. Aamo, Department of Engineering Cybernetics, Norwegian University of Science and Technology, N-7491 Trondheim, Norway. E-mail: aamo@itk.ntnu.no

Received 21 March 2002; Accepted 16 November 2003.
Recommended by D. Normand-Cyrot and A. van der Schaft.

a third actuation slot, shedding was reduced considerably, even at $R = 80$.

Although some success in controlling vortex shedding has been achieved in numerical simulations, rigorous control designs are scarce due to the complexity of designing controllers based on the Navier–Stokes equation. A much simpler model, the Ginzburg–Landau equation with appropriate coefficients, has been found to model well the dynamics of vortex shedding near the critical value of the Reynolds number [8]. In [12], it was shown numerically that the Ginzburg–Landau model for Reynolds numbers close to R_c can be stabilized using proportional feedback from a single measurement downstream of the cylinder, to local forcing at the location of the cylinder. In [10], using the model from [12], stabilization was obtained in numerical simulations for $R = 100$, with an LQG controller designed for the linearized Ginzburg–Landau equation. The actuation can be effected in a number of different ways, including wall transpiration, as suggested in [7,11] and transverse cylinder oscillations or loudspeakers, as suggested in [12]. On a more general note, approaches for controlling nonlinear parabolic PDEs include [2,3].

In this paper, we design a controller using backstepping, that is shown to globally stabilize the equilibrium at zero of a finite difference discretization of any order of the nonlinear Ginzburg–Landau model presented in [12]. This method is similar to that used for global stabilization of a thermal convection loop in [3], stabilization of a solid propellant rocket instability in [4], and boundary control for chemical tubular reactors in [5]. The method is different from previous control designs for the Ginzburg–Landau model in that it provides a global stability result (valid for any initial state), as opposed to the local results achieved by linearization in [10]. The control design is valid for any Reynolds number, although the model is only valid for Reynolds numbers close to the critical value $R_c = 47$. Numerical simulations are provided in order to demonstrate the performance of the controller, along with the potential of using low order discretizations for the control design, and thereby reducing the number of sensors needed for implementation.

2. Problem Formulation

The Ginzburg–Landau equation in the notation of [12] is given by

$$\frac{\partial A}{\partial t} = -a_1(x)\frac{\partial A}{\partial x} - a_2\frac{\partial^2 A}{\partial x^2} - a_4(x)A + a_5|A|^2A + \delta(x - x_a)u, \tag{1}$$

where $x \in \mathbb{R}$, $A : \mathbb{R} \times \mathbb{R}_+ \to \mathbb{C}$, $a_1, a_4 : \mathbb{R} \to \mathbb{C}$, and $a_2, a_5 \in \mathbb{C}$. δ denotes the Dirac distribution and $u : \mathbb{R}_+ \to \mathbb{C}$ is the control input. Thus, control input is in the form of local forcing at x_a. The boundary conditions are $A(x \to \pm\infty, t) = 0$, i.e., homogeneous Dirichlet boundary conditions. The following holds for the coefficients of (1).

Assumption 1. $a_2 \in (\infty, 0)$ and $\Re(a_5) \in (-\infty, 0]$.

We now rewrite the equation to obtain two coupled partial differential equations in real variables and coefficients by defining

$$\rho \triangleq \tfrac{1}{2}(A + \bar{A}), \quad \iota \triangleq \frac{1}{2\mathrm{i}}(A - \bar{A}), \tag{2}$$

$$a_{R_j} \triangleq \tfrac{1}{2}(a_j + \bar{a}_j), \quad a_{I_j} \triangleq \frac{1}{2\mathrm{i}}(a_j - \bar{a}_j), \quad j = 1,2,4,5, \tag{3}$$

$$u_R \triangleq \tfrac{1}{2}(u + \bar{u}), \quad u_I \triangleq \frac{1}{2\mathrm{i}}(u - \bar{u}), \tag{4}$$

where i denotes the imaginary unit and $-$ denotes complex conjugation. With these definitions we obtain

$$\begin{aligned}
\frac{\partial \rho}{\partial t} &= \frac{1}{2}\left(\frac{\partial A}{\partial t} + \frac{\partial \bar{A}}{\partial t}\right) \\
&= \frac{1}{2}\Bigg(-(a_{R_1} + \mathrm{i}a_{I_1})\left(\frac{\partial \rho}{\partial x} + \mathrm{i}\frac{\partial \iota}{\partial x}\right) \\
&\quad - (a_{R_2} + \mathrm{i}a_{I_2})\left(\frac{\partial^2 \rho}{\partial x^2} + \mathrm{i}\frac{\partial^2 \iota}{\partial x^2}\right) \\
&\quad - (a_{R_4} + \mathrm{i}a_{I_4})(\rho + \mathrm{i}\iota) + (a_{R_5} + \mathrm{i}a_{I_5})|A|^2(\rho + \mathrm{i}\iota) \\
&\quad + \delta(x - x_a)(u_R + \mathrm{i}u_I) \\
&\quad - (a_{R_1} - \mathrm{i}a_{I_1})\left(\frac{\partial \rho}{\partial x} - \mathrm{i}\frac{\partial \iota}{\partial x}\right) \\
&\quad - (a_{R_2} - \mathrm{i}a_{I_2})\left(\frac{\partial^2 \rho}{\partial x^2} - \mathrm{i}\frac{\partial^2 \iota}{\partial x^2}\right) \\
&\quad - (a_{R_4} - \mathrm{i}a_{I_4})(\rho - \mathrm{i}\iota) + (a_{R_5} - \mathrm{i}a_{I_5})|A|^2(\rho - \mathrm{i}\iota) \\
&\quad + \delta(x - x_a)(u_R - \mathrm{i}u_I)\Bigg) \\
&= -a_{R_1}(x)\frac{\partial \rho}{\partial x} + a_{I_1}(x)\frac{\partial \iota}{\partial x} - a_{R_2}\frac{\partial^2 \rho}{\partial x^2} + a_{I_2}\frac{\partial^2 \iota}{\partial x^2} \\
&\quad - a_{R_4}(x)\rho + a_{I_4}(x)\iota + |A|^2 a_{R_5}\rho - |A|^2 a_{I_5}\iota \\
&\quad + \delta(x - x_a)u_R
\end{aligned} \tag{5}$$

and

$$\begin{aligned}\frac{\partial \iota}{\partial t} &= \frac{1}{2\mathrm{i}}\left(\frac{\partial A}{\partial t} - \frac{\partial \bar{A}}{\partial t}\right)\\ &= \frac{1}{2\mathrm{i}}\Bigg(-(a_{R_1}+\mathrm{i}a_{I_1})\left(\frac{\partial \rho}{\partial x}+\mathrm{i}\frac{\partial \iota}{\partial x}\right)\\ &\quad -(a_{R_2}+\mathrm{i}a_{I_2})\left(\frac{\partial^2 \rho}{\partial x^2}+\mathrm{i}\frac{\partial^2 \iota}{\partial x^2}\right)\\ &\quad -(a_{R_4}+\mathrm{i}a_{I_4})(\rho+\mathrm{i}\iota)+(a_{R_5}+\mathrm{i}a_{I_5})|A|^2(\rho+\mathrm{i}\iota)\\ &\quad +\delta(x-x_a)(u_R+\mathrm{i}u_I)+(a_{R_1}-\mathrm{i}a_{I_1})\left(\frac{\partial \rho}{\partial x}-\mathrm{i}\frac{\partial \iota}{\partial x}\right)\\ &\quad +(a_{R_2}-\mathrm{i}a_{I_2})\left(\frac{\partial^2 \rho}{\partial x^2}-\mathrm{i}\frac{\partial^2 \iota}{\partial x^2}\right)+(a_{R_4}-\mathrm{i}a_{I_4})(\rho-\mathrm{i}\iota)\\ &\quad -(a_{R_5}-\mathrm{i}a_{I_5})|A|^2(\rho-\mathrm{i}\iota)-\delta(x-x_a)(u_R-\mathrm{i}u_I)\Bigg)\\ &= -a_{R_1}(x)\frac{\partial \iota}{\partial x}-a_{I_1}(x)\frac{\partial \rho}{\partial x}-a_{R_2}\frac{\partial^2 \iota}{\partial x^2}-a_{I_2}\frac{\partial^2 \rho}{\partial x^2}\\ &\quad -a_{R_4}(x)\iota-a_{I_4}(x)\rho+|A|^2a_{R_5}\iota+|A|^2a_{I_5}\rho\\ &\quad +\delta(x-x_a)u_1. \qquad (6)\end{aligned}$$

Rearranging the terms, the equations become

$$\begin{aligned}\frac{\partial \rho}{\partial t} &= -\left(a_{R_1}(x)\frac{\partial}{\partial x}+a_{R_2}\frac{\partial^2}{\partial x^2}+a_{R_4}(x)-a_{R_5}(\rho^2+\iota^2)\right)\rho\\ &\quad +\left(a_{I_1}(x)\frac{\partial}{\partial x}+a_{I_2}\frac{\partial^2}{\partial x^2}+a_{I_4}(x)-a_{I_5}(\rho^2+\iota^2)\right)\iota\\ &\quad +\delta(x-x_a)u_R, \qquad (7)\end{aligned}$$

$$\begin{aligned}\frac{\partial \iota}{\partial t} &= -\left(a_{I_1}(x)\frac{\partial}{\partial x}+a_{I_2}\frac{\partial^2}{\partial x^2}+a_{I_4}(x)-a_{I_5}(\rho^2+\iota^2)\right)\rho\\ &\quad -\left(a_{R_1}(x)\frac{\partial}{\partial x}+a_{R_2}\frac{\partial^2}{\partial x^2}+a_{R_4}(x)-a_{R_5}(\rho^2+\iota^2)\right)\iota\\ &\quad +\delta(x-x_a)u_I, \qquad (8)\end{aligned}$$

with boundary conditions $\rho(\infty,t)=0$ and $\iota(\pm\infty,t)=0$. In view of Assumption 1 we have $a_{R_2}<0$, $a_{I_2}=0$, and $a_{R_5}\le 0$. Equations (7) and (8), with numerical values as given in [12, Appendix A] (reproduced in Appendix A), have been found to model well the dynamics of vortex shedding from a circular cylinder at Reynolds numbers near the critical Reynolds number, R_c. Based on the numerical values given in [12, Appendix A], we state the following assumption, which is assumed to hold throughout the analysis that follows.

Assumption 2. For $|x|\gg 0$,

$$\frac{1}{4a_{R_2}}a_{I_1}^2(x)+a_{R_4}(x)\sim x^2. \qquad (9)$$

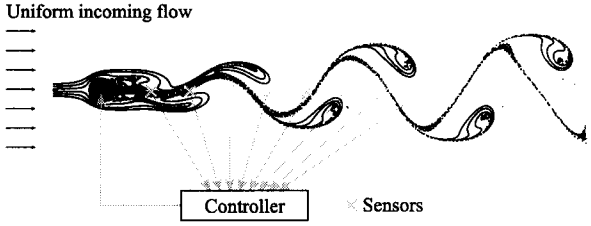

Fig. 1. Vortex shedding from a cylinder visualized by passive tracer particles [1]. The figure also shows the proposed control system configuration for suppression of vortex shedding.

We will design a control law that stabilizes the zero-solution of a finite difference approximation of (7)–(8) on a bounded subdomain, and the zero-solution of the PDE (7)–(8) in L_2-norm outside the subdomain. Figure 1 shows a sketch of the control system, along with a visualization of vortex shedding. Existence, uniqueness, and regularity of solutions of the closed loop system for large initial data is far harder than the problem of control design, and remains an open problem. We refer the reader to [13] for a treatment of these issues in the case of the uncontrolled Ginzburg–Landau equation with constant parameters.

3. Main Results

The basic idea of the control design is to divide the domain into three separate parts; the upstream subsystem, defined on $(-\infty, x_u)$, the core, defined on $[x_u, x_d]$, and the downstream subsystem, defined on (x_d, ∞), for which the following two facts are shown:

1. The upstream and downstream subsystems are input-to-state stable (in L_2 norm) with respect to certain boundary input terms.
2. A finite-difference approximation of any order of the core can be stabilized by state feedback, driving all the states to zero, including the boundary input terms of the upstream and downstream subsystems.

These two facts are treated in detail in Sections 3.1 and 3.2, respectively.

3.1. Energy Analysis

Lemma 3. There exist real constants $x_u<0$ and $x_d>0$ such that solutions of system (7)–(8) satisfy

$$\begin{aligned}&\frac{\mathrm{d}}{\mathrm{d}t}\left(\|(\rho,\iota)\|^2_{L_2(-\infty,x_u)}\right)\\ &\quad \le -c\|(\rho,\iota)\|^2_{L_2(-\infty,x_u)}-\Bigg(a_{R_1}(x)(\rho^2+\iota^2)\\ &\qquad +2a_{R_2}\left(\frac{\partial \rho}{\partial x}\rho+\frac{\partial \iota}{\partial x}\iota\right)\Bigg)\Bigg|_{x=x_u} \qquad (10)\end{aligned}$$

$$\frac{\mathrm{d}}{\mathrm{d}t}\left(\|(\rho,\iota)\|^2_{L_2(x_\mathrm{d},\infty)}\right)$$
$$\leq -c\|(\rho,\iota)\|^2_{L_2(x_\mathrm{d},\infty)} + \left(a_{R_1}(x)(\rho^2+\iota^2) + 2a_{R_2}\left(\frac{\partial\rho}{\partial x}\rho+\frac{\partial\iota}{\partial x}\iota\right)\right)\Bigg|_{x=x_\mathrm{d}} \tag{11}$$

for some positive constant c.

Proof. The time derivative of $\|(\rho,\iota)\|^2_{L_2(a,b)}$ along solutions of (7)–(8) is

$$\frac{\mathrm{d}}{dt}\left(\|(\rho,\iota)\|^2_{L_2(a,b)}\right)$$
$$= 2\int_a^b (\rho\dot\rho+\iota\dot\iota)\,\mathrm{d}x$$
$$= 2\int_a^b \Big[-\Big(a_{R_1}(x)\frac{\partial\rho}{\partial x}+a_{R_2}\frac{\partial^2\rho}{\partial x^2}+a_{R_4}(x)\rho-|A|^2a_{R_5}\rho\Big)\rho + \Big(a_{I_1}(x)\frac{\partial\iota}{\partial x}+a_{I_2}\frac{\partial^2\iota}{\partial x^2}\Big)\rho-\Big(a_{I_1}(x)\frac{\partial\rho}{\partial x}+a_{I_2}\frac{\partial^2\rho}{\partial x^2}\Big)\iota - \Big(a_{R_1}(x)\frac{\partial\iota}{\partial x}+a_{R_2}\frac{\partial^2\iota}{\partial x^2}+a_{R_4}(x)\iota-|A|^2a_{R_5}\iota\Big)\iota\Big]\,\mathrm{d}x, \tag{12}$$

where $a<b$ are constants satisfying $x_\mathrm{a}\notin(a,b)$. Integration by parts yields

$$-2\int_a^b a_{R_1}(x)\frac{\partial\rho}{\partial x}\rho\,\mathrm{d}x = -\left[a_{R_1}(x)\rho^2\right]_a^b+\int_a^b\frac{\partial a_{R_1}}{\partial x}\rho^2\,\mathrm{d}x \tag{13}$$
$$-2\int_a^b a_{R_1}(x)\frac{\partial\iota}{\partial x}\iota\,\mathrm{d}x = -\left[a_{R_1}(x)\iota^2\right]_a^b+\int_a^b\frac{\partial a_{R_1}}{\partial x}\iota^2\,\mathrm{d}x \tag{14}$$
$$-2\int_a^b a_{R_2}\frac{\partial^2\rho}{\partial x^2}\rho\,\mathrm{d}x = -2\left[a_{R_2}\frac{\partial\rho}{\partial x}\rho\right]_a^b+2\int_a^b a_{R_2}\left(\frac{\partial\rho}{\partial x}\right)^2\mathrm{d}x \tag{15}$$
$$-2\int_a^b a_{R_2}\frac{\partial^2\iota}{\partial x^2}\iota\,\mathrm{d}x = -2\left[a_{R_2}\frac{\partial\iota}{\partial x}\iota\right]_a^b+2\int_a^b a_{R_2}\left(\frac{\partial\iota}{\partial x}\right)^2\mathrm{d}x. \tag{16}$$

Inserting (13)–(16) into (12), keeping in mind that $a_{I_2}=0$ and $a_{R_5}\leq 0$ (Assumption 1), yields

$$\frac{\mathrm{d}}{\mathrm{d}t}\left(\|(\rho,\iota)\|^2_{L_2(a,b)}\right) \leq \left[-a_{R_1}(x)(\rho^2+\iota^2)-2a_{R_2}\left(\frac{\partial\rho}{\partial x}\rho+\frac{\partial\iota}{\partial x}\iota\right)\right]_a^b + 2\int_a^b\Big[a_{R_2}\left(\frac{\partial\iota}{\partial x}\right)^2+a_{I_1}(x)\frac{\partial\iota}{\partial x}\rho-\left(-\frac{\partial a_{R_1}}{\partial x}+a_{R_4}(x)\right)\rho^2 + a_{R_2}\left(\frac{\partial\rho}{\partial x}\right)^2-a_{I_1}(x)\frac{\partial\rho}{\partial x}\iota-\left(-\frac{\partial a_{R_1}}{\partial x}+a_{R_4}(x)\right)\iota^2\Big]\,\mathrm{d}x. \tag{17}$$

Now, consider the integrand in (17). We have that

$$a_{R_2}\left(\frac{\partial\iota}{\partial x}\right)^2+a_{I_1}(x)\frac{\partial\iota}{\partial x}\rho-\left(-\frac{\partial a_{R_1}}{\partial x}+a_{R_4}(x)\right)\rho^2 + a_{R_2}\left(\frac{\partial\rho}{\partial x}\right)^2-a_{I_1}(x)\frac{\partial\rho}{\partial x}\iota-\left(-\frac{\partial a_{R_1}}{\partial x}+a_{R_4}(x)\right)\iota^2$$
$$\leq a_{R_2}\left|\frac{\partial\iota}{\partial x}\right|^2+|a_{I_1}(x)|\left|\frac{\partial\iota}{\partial x}\right||\rho|-\left(-\frac{\partial a_{R_1}}{\partial x}+a_{R_4}(x)\right)\rho^2 + a_{R_2}\left|\frac{\partial\rho}{\partial x}\right|^2+|a_{I_1}(x)|\left|\frac{\partial\rho}{\partial x}\right||\iota|-\left(-\frac{\partial a_{R_1}}{\partial x}+a_{R_4}(x)\right)\iota^2$$
$$= a_{R_2}\left(\left|\frac{\partial\iota}{\partial x}\right|+\frac{1}{2a_{R_2}}|a_{I_1}(x)||\rho|\right)^2 - \left(\frac{1}{4a_{R_2}}a_{I_1}^2(x)-\frac{\partial a_{R_1}}{\partial x}+a_{R_4}(x)\right)\rho^2 + a_{R_2}\left(\left|\frac{\partial\rho}{\partial x}\right|+\frac{1}{2a_{R_2}}|a_{I_1}(x)||\iota|\right)^2 - \left(\frac{1}{4a_{R_2}}a_{I_1}^2(x)-\frac{\partial a_{R_1}}{\partial x}+a_{R_4}(x)\right)\iota^2$$
$$\leq -\left(\frac{1}{4a_{R_2}}a_{I_1}^2(x)-\frac{\partial a_{R_1}}{\partial x}+a_{R_4}(x)\right)(\rho^2+\iota^2), \tag{18}$$

where we have used the fact that $a_{R_2}<0$ (Assumption 1). Inserting (18) into (17) we obtain

$$\frac{\mathrm{d}}{\mathrm{d}t}\left(\|(\rho,\iota)\|^2_{L_2(a,b)}\right) \leq \left[-a_{R_1}(x)(\rho^2+\iota^2)-2a_{R_2}\left(\frac{\partial\rho}{\partial x}\rho+\frac{\partial\iota}{\partial x}\iota\right)\right]_a^b - 2\int_a^b\left(\frac{1}{4a_{R_2}}a_{I_1}^2(x)-\frac{\partial a_{R_1}}{\partial x}+a_{R_4}(x)\right)(\rho^2+\iota^2)\,\mathrm{d}x. \tag{19}$$

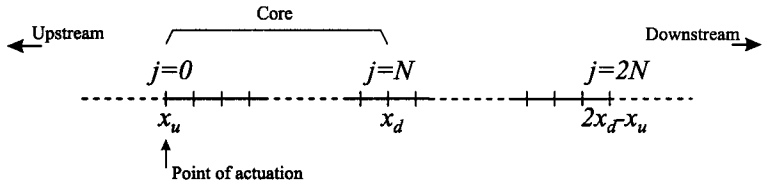

Fig. 2. The system is discretized in the interval $[x_u, 2x_d - x_u]$, using a uniform grid with cell size h.

By Assumption 2 there exist positive constants $x_u < 0$, and $x_d > 0$, and $c > 0$, such that

$$\left(\frac{1}{4a_{R_2}}a_{I_1}^2(x) - \frac{\partial a_{R_1}}{\partial x} + a_{R_4}(x)\right) > \frac{1}{2}c, \quad \text{for } x \in (-\infty, x_u) \cup (x_d, \infty). \tag{20}$$

Inserting (20) into (19), (10) and (11) now follow by picking $(a, b) = (-\infty, x_u)$ and $(a, b) = (x_d, \infty)$, respectively, and applying the boundary conditions at $x = \pm\infty$.

3.2. Stabilization by State Feedback

3.2.1. Discretization

Having determined the two constants x_u and x_d, which exist by Lemma 3, we discretize (7)–(8) using finite difference approximations on the interval $[x_u, 2x_d - x_u]$ as shown schematically in Fig. 2. We define the finite difference approximations

$$\frac{\partial \rho}{\partial x}(jh) \approx \frac{\rho((j+1)h) - \rho(jh)}{h} \triangleq \frac{1}{h}\rho_{j+1} - \frac{1}{h}\rho_j, \tag{21}$$

$$\frac{\partial^2 \rho}{\partial x^2} \approx \frac{\rho((j+1)h) - 2\rho(jh) + \rho((j-1)h)}{h^2} \triangleq \frac{\rho_{j+1}}{h^2} - 2\frac{\rho_j}{h^2} + \frac{\rho_{j-1}}{h^2}, \tag{22}$$

$$\frac{\partial \iota}{\partial x}(jh) \approx \frac{\iota((j+1)h) - \iota(jh)}{h} \triangleq \frac{1}{h}\iota_{j+1} - \frac{1}{h}\iota_j, \tag{23}$$

$$\frac{\partial^2 \iota}{\partial x^2} \approx \frac{\iota((j+1)h) - 2\iota(jh) + \iota((j-1)h)}{h^2} \triangleq \frac{\iota_{j+1}}{h^2} - 2\frac{\iota_j}{h^2} + \frac{\iota_{j-1}}{h^2}, \tag{24}$$

and to simplify notation we set

$$r_{1,j} = a_{R_1}(x_j), \tag{25}$$

$$i_{1,j} = a_{I_1}(x_j), \tag{26}$$

$$r_2 = \frac{a_{R_2}}{h}, \tag{27}$$

$$r_{3,j} = h a_{R_4}(x_j), \tag{28}$$

$$i_{3,j} = h a_{I_4}(x_j), \tag{29}$$

$$r_4 = h a_{R_5}, \tag{30}$$

$$i_4 = h a_{I_5}. \tag{31}$$

Inserting (21)–(31) into (7)–(8) we obtain the set of ordinary differential equations:

$$\begin{aligned} h\dot{\rho}_j = &-r_2\rho_{j-1} + (r_{1,j} + 2r_2 - r_{3,j} + r_4(\rho_j^2 + \iota_j^2))\rho_j \\ &- (r_{1,j} + r_2)\rho_{j+1} + (-i_{1,j} + i_{3,j} - i_4(\rho_j^2 + \iota_j^2))\iota_j \\ &+ i_{1,j}\iota_{j+1} + \delta_{0,j}u_R, \end{aligned} \tag{32}$$

$$\begin{aligned} h\dot{\iota}_j = &(i_{1,j} - i_{3,j} + i_4(\rho_j^2 + \iota_j^2))\rho_j - i_{1,j}\rho_{j+1} - r_2\iota_{j-1} \\ &+ (r_{1,j} + 2r_2 - r_{3,j} + r_4(\rho_j^2 + \iota_j^2))\iota_j \\ &- (r_{1,j} + r_2)\iota_{j+1} + \delta_{0,j}u_I, \end{aligned} \tag{33}$$

for $j = 0, 1, 2, \ldots, 2N+2$, where $x_j \triangleq hj + x_u$ and $\delta_{i,j}$ denotes the Kronecker delta function. In (32)–(33) we have set the point of actuation to $x_a = x_u$, and used the fact that $a_{I_2} = 0$. Inserting (21)–(31) into (10) and (11) we obtain

$$\begin{aligned} &\frac{d}{dt}\left(\|(\rho, \iota)\|^2_{L_2(-\infty, x_u)}\right) \\ &\quad \le -c\|(\rho, \iota)\|^2_{L_2(-\infty, x_u)} - r_{1,0}(\rho_0^2 + \iota_0^2) \\ &\qquad - 2r_2((\rho_1 - \rho_0)\rho_0 + (\iota_1 - \iota_0)\iota_0) \end{aligned} \tag{34}$$

and

$$\begin{aligned} &\frac{d}{dt}\left(\|(\rho, \iota)\|^2_{L_2(x_d, \infty)}\right) \\ &\quad \le -c|(\rho, \iota)|^2_{L_2(x_d, \infty)} + r_{1,N}(\rho_N^2 + \iota_N^2) \\ &\qquad + 2r_2((\rho_{N+1} - \rho_N)\rho_N + (\iota_{N+1} - \iota_N)\iota_N), \end{aligned} \tag{35}$$

which are the semi-discrete versions of (10)–(11). The reason why the discretization is carried out on $[x_u, 2x_d - x_u]$, rather than just the core $[x_u, x_d]$, will be explained in a remark following the results presented in the next section.

3.2.2. Control Design

The following theorem summarizes our control design.

Theorem 4. The control law defined recursively by the scheme

$$\alpha_N \equiv \beta_N \equiv 0, \tag{36}$$

$$\alpha_{N-1}(\rho_N, \rho_{N+1}, \iota_{N+1}) = \frac{1}{r_2}\left[\left(\frac{3}{2}r_{1,N} - r_{3,N} + c_N\right)\rho_N - r_{1,N}\rho_{N+1} + i_{1,N}\iota_{N+1}\right], \tag{37}$$

$$\beta_{N-1}(\rho_{N+1}, \iota_N, \iota_{N+1}) = \frac{1}{r_2}\left[-i_{1,N}\rho_{N+1} + \left(\frac{3}{2}r_{1,N} - r_{3,N} + c_N\right)\iota_N - r_{1,N}\iota_{N+1}\right], \tag{38}$$

$$\begin{aligned}
&\alpha_{N-k}(\rho_j, \iota_j : j \in [N-k+1, N+k]) \\
&= \frac{1}{r_2}[c_{N-(k-1)}(\rho_{N-(k-1)} - \alpha_{N-(k-1)}) \\
&\quad + (r_{1,N-(k-1)} + 2r_2 - r_{3,N-(k-1)} \\
&\quad + r_4(\rho^2_{N-(k-1)} + \iota^2_{N-(k-1)}))\rho_{N-(k-1)} \\
&\quad - (r_{1,N-(k-1)} + 2r_2)\rho_{N-(k-2)} + (-i_{1,N-(k-1)} + i_{3,N-(k-1)} \\
&\quad - i_4(\rho^2_{N-(k-1)} + \iota^2_{N-(k-1)}))\iota_{N-(k-1)} + i_{1,N-(k-1)}\iota_{N-(k-2)} \\
&\quad + r_2\alpha_{N-(k-2)} - \sum_{j=N-k+2}^{N+k-1} \frac{\partial \alpha_{N-(k-1)}}{\partial \rho_j} \\
&\quad \times (-r_2\rho_{j-1} + (r_{1,j} + 2r_2 - r_{3,j} + r_4(\rho_j^2 + \iota_j^2))\rho_j \\
&\quad - (r_{1,j} + r_2)\rho_{j+1} + (-i_{1,j} + i_{3,j} - i_4(\rho_j^2 + \iota_j^2))\iota_j + i_{1,j}\iota_{j+1}) \\
&\quad - \sum_{j=N-k+2}^{N+k-1} \frac{\partial \alpha_{N-(k-1)}}{\partial \iota_j}((i_{1,j} - i_{3,j} + i_4(\rho_j^2 + \iota_j^2))\rho_j - i_{1,j}\rho_{j+1} \\
&\quad - r_2\iota_{j-1} + (r_{1,j} + 2r_2 - r_{3,j} + r_4(\rho_j^2 + \iota_j^2))\iota_j \\
&\quad - (r_{1,j} + r_2)\iota_{j+1})]
\end{aligned} \tag{39}$$

$$\begin{aligned}
&\beta_{N-k}(\rho_j, \iota_j : j \in [N-k+1, N+k]) \\
&= \frac{1}{r_2}[c_{N-(k-1)}(\iota_{N-(k-1)} - \beta_{N-(k-1)}) \\
&\quad + (i_{1,N-(k-1)} - i_{3,N-(k-1)} \\
&\quad + i_4(\rho^2_{N-(k-1)} + \iota^2_{N-(k-1)}))\rho_{N-(k-1)} \\
&\quad - i_{1,N-(k-1)}\rho_{N-(k-2)} \\
&\quad + (r_{1,N-(k-1)} + 2r_2 - r_{3,N-(k-1)} \\
&\quad + r_4(\rho^2_{N-(k-1)} + \iota^2_{N-(k-1)}))\iota_{N-(k-1)} \\
&\quad - (r_{1,N-(k-1)} + 2r_2)\iota_{N-(k-2)} + r_2\beta_{N-(k-2)} \\
&\quad - \sum_{j=N-k+2}^{N+k-1} \frac{\partial \beta_{N-(k-1)}}{\partial \rho_j}(-r_2\rho_{j-1} + (r_{1,j} + 2r_2 - r_{3,j} \\
&\quad + r_4(\rho_j^2 + \iota_j^2))\rho_j - (r_{1,j} + r_2)\rho_{j+1} + (-i_{1,j} + i_{3,j} \\
&\quad - i_4(\rho_j^2 + \iota_j^2))\iota_j + i_{1,j}\iota_{j+1}) - \sum_{j=N-k+2}^{N+k-1} \frac{\partial \beta_{N-(k-1)}}{\partial \iota_j} \\
&\quad \times ((i_{1,j} - i_{3,j} + i_4(\rho_j^2 + \iota_j^2))\rho_j - i_{1,j}\rho_{j+1} - r_2\iota_{j-1} \\
&\quad + (r_{1,j} + 2r_2 - r_{3,j} + r_4(\rho_j^2 + \iota_j^2))\iota_j - (r_{1,j} + r_2)\iota_{j+1})]
\end{aligned} \tag{40}$$

for $k = 2, 3, 4, \ldots, N$, and

$$\begin{aligned}
&u_R(\rho_j, \iota_j : j \in [-1, 2N+1]) \\
&= -[c_0(\rho_0 - \alpha_0) - r_2\rho_{-1} \\
&\quad + (r_{1,0} + 2r_2 - r_{3,0} + r_4(\rho_0^2 + \iota_0^2))\rho_0 \\
&\quad - (r_{1,0} + 2r_2)\rho_1 + (-i_{1,0} + i_{3,0} - i_4(\rho_0^2 + \iota_0^2))\iota_0 \\
&\quad + i_{1,0}\iota_1 + r_2\alpha_1 - \sum_{j=1}^{2N} \frac{\partial \alpha_0}{\partial \rho_j}(-r_2\rho_{j-1} \\
&\quad + (r_{1,j} + 2r_2 - r_{3,j} + r_4(\rho_j^2 + \iota_j^2))\rho_j \\
&\quad - (r_{1,j} + r_2)\rho_{j+1} + (-i_{1,j} + i_{3,j} - i_4(\rho_j^2 + \iota_j^2))\iota_j \\
&\quad + i_{1,j}\iota_{j+1}) - \sum_{j=1}^{2N} \frac{\partial \alpha_0}{\partial \iota_j}((i_{1,j} - i_{3,j} + i_4(\rho_j^2 + \iota_j^2))\rho_j \\
&\quad - i_{1,j}\rho_{j+1} - r_2\iota_{j-1} + (r_{1,j} + 2r_2 - r_{3,j} \\
&\quad + r_4(\rho_j^2 + \iota_j^2))\iota_j - (r_{1,j} + r_2)\iota_{j+1})]
\end{aligned} \tag{41}$$

$$\begin{aligned}
&u_I(\rho_j, \iota_j : j \in [-1, 2N+1]) \\
&= -[c_0(\iota_0 - \beta_0) + (i_{1,0} - i_{3,0} + i_4(\rho_0^2 + \iota_0^2))\rho_0 - i_{1,0}\rho_1 \\
&\quad - r_2\iota_{-1} + (r_{1,0} + 2r_2 - r_{3,0} + r_4(\rho_0^2 + \iota_0^2))\iota_0 \\
&\quad - (r_{1,0} + 2r_2)\iota_1 + r_2\beta_1 - \sum_{j=1}^{2N} \frac{\partial \beta_0}{\partial \rho_j}(-r_2\rho_{j-1} \\
&\quad + (r_{1,j} + 2r_2 - r_{3,j} + r_4(\rho_j^2 + \iota_j^2))\rho_j \\
&\quad - (r_{1,j} + r_2)\rho_{j+1} + (-i_{1,j} + i_{3,j} - i_4(\rho_j^2 + \iota_j^2))\iota_j + i_{1,j}\iota_{j+1}) \\
&\quad - \sum_{j=1}^{2N} \frac{\partial \beta_0}{\partial \iota_j}((i_{1,j} - i_{3,j} + i_4(\rho_j^2 + \iota_j^2))\rho_j - i_{1,j}\rho_{j+1} - r_2\iota_{j-1} \\
&\quad + (r_{1,j} + 2r_2 - r_{3,j} + r_4(\rho_j^2 + \iota_j^2))\iota_j - (r_{1,j} + r_2)\iota_{j+1})],
\end{aligned} \tag{42}$$

renders $(\rho_0, \iota_0, \rho_1, \iota_1, \ldots, \rho_N, \iota_N) = 0$ globally asymptotically stable. Moreover, solutions of system (7)–(8) satisfy

$$\|(\rho, \iota)\|^2_{L_2(-\infty, x_u)} \to 0, \tag{43}$$

$$\|(\rho, \iota)\|^2_{L_2(x_d, \infty)} \to 0, \tag{44}$$

as $t \to \infty$.

Proof. Consider the Lyapunov function candidate

$$V = \frac{h}{2}\sum_{j=0}^{N}\left[(\rho_j - \alpha_j)^2 + (\iota_j - \beta_j)^2\right] + \frac{1}{2}\|(\rho, \iota)\|_{L_2(x_d, \infty)}. \tag{45}$$

The time derivative of (45) along solutions of the system is

$$\dot V = \sum_{j=0}^{N-1}\left[(\rho_j - \alpha_j)(h\dot\rho_j - h\dot\alpha_j) + (\iota_j - \beta_j)(hi_j - h\dot\beta_j)\right] + (\rho_N h\dot\rho_N + \iota_N h i_N) + \frac{1}{2}\frac{\mathrm{d}}{\mathrm{d}t}\left[\|(\rho, \iota)\|^2_{L_2(x_d, \infty)}\right], \tag{46}$$

where we have used the fact that $\alpha_N = \beta_N = 0$. Inserting (37)–(38) into (46), yields

$$\begin{aligned}\dot V \le{}& \sum_{j=0}^{N-1}\left[(\rho_j - \alpha_j)(h\dot\rho_j - h\dot\alpha_j) + (\iota_j - \beta_j)(hi_j - h\dot\beta_j)\right] \\ &- r_2\rho_N(\rho_{N-1} - \alpha_{N-1}) - r_2\iota_N(\iota_{N-1} - r_2\beta_{N-1}) \\ &- (c_N - r_2)(\rho_N^2 + \iota_N^2) + r_4(\rho_N^2 + \iota_N^2)^2 \\ &- \frac{c}{2}\|(\rho, \iota)\|^2_{L_2(x_d, \infty)} \\ \le{}& \sum_{j=0}^{N-1}\left[(\rho_j - \alpha_j)(h\dot\rho_j - h\dot\alpha_j) + (\iota_j - \beta_j)(hi_j - h\dot\beta_j)\right] \\ &- r_2\rho_N(\rho_{N-1} - \alpha_{N-1}) - r_2\iota_N(\iota_{N-1} - \beta_{N-1}) \\ &- (c_N - r_2)(\rho_N^2 + \iota_N^2) - \frac{c}{2}\|(\rho, \iota)\|^2_{L_2(x_d, \infty)},\end{aligned} \tag{47}$$

where we have used the fact that $r_4 < 0$ (Assumption 1) in the last step. Next, we insert (32)–(33) into (47), and obtain

$$\begin{aligned}\dot V \le{}& (\rho_0 - \alpha_0)[-r_2\rho_{-1} + (r_{1,0} + 2r_2 - r_{3,0} \\ &+ r_4(\rho_0^2 + \iota_0^2))\rho_0 - (r_{1,0} + r_2)\rho_1 \\ &+ (-i_{1,0} + i_{3,0} - i_4(\rho_0^2 + \iota_0^2))\iota_0 \\ &+ i_{1,0}\iota_1 + u_R - h\dot\alpha_0] \\ &+ (\iota_0 - \beta_0)[(i_{1,0} - i_{3,0} + i_4(\rho_0^2 + \iota_0^2))\rho_0 \\ &- i_{1,0}\rho_1 - r_2\iota_{-1} \\ &+ (r_{1,0} + 2r_2 - r_{3,0} + r_4(\rho_0^2 + \iota_0^2))\iota_0 \\ &- (r_{1,0} + r_2)\iota_1 + u_I - h\dot\beta_0] \\ &+ \sum_{j=1}^{N-1}[(\rho_j - \alpha_j)(-r_2\rho_{j-1} + (r_{1,j} + 2r_2 - r_{3,j} + r_4(\rho_j^2 + \iota_j^2))\rho_j \\ &- (r_{1,j} + r_2)\rho_{j+1} \\ &+ (-i_{1,j} + i_{3,j} - i_4(\rho_j^2 + \iota_j^2))\iota_j \\ &+ i_{1,j}\iota_{j+1} - h\dot\alpha_j) \\ &+ (\iota_j - \beta_j)((i_{1,j} - i_{3,j} + i_4(\rho_j^2 + \iota_j^2))\rho_j \\ &- i_{1,j}\rho_{j+1} - r_2\iota_{j-1} \\ &+ (r_{1,j} + 2r_2 - r_{3,j} + r_4(\rho_j^2 + \iota_j^2))\iota_j \\ &- (r_{1,j} + r_2)\iota_{j+1} - h\dot\beta_j)] \\ &- r_2\rho_N(\rho_{N-1} - \alpha_{N-1}) - r_2\iota_N(\iota_{N-1} - \beta_{N-1}) \\ &- (c_N - r_2)(\rho_N^2 + \iota_N^2) - \frac{c}{2}\|(\rho, \iota)\|^2_{L_2(x_d, \infty)}.\end{aligned} \tag{48}$$

At this point, we observe that the two summations in (39) in fact equal the time derivative of the previous α multiplied by h, that is $h\dot\alpha_{N-(k-1)}$. Similarly, the two summations in (40) equal the time derivative of the previous β multiplied by h, that is $h\dot\beta_{N-(k-1)}$. Therefore, from (39)–(40) we have

$$\begin{aligned}h\dot\alpha_j = {}& c_j(\rho_j - \alpha_j) - r_2\alpha_{j-1} + (r_{1,j} + 2r_2 - r_{3,j} + r_4(\rho_j^2 + \iota_j^2))\rho_j \\ &- (r_{1,j} + 2r_2)\rho_{j+1} + (-i_{1,j} + i_{3,j} - i_4(\rho_j^2 + \iota_j^2))\iota_j \\ &+ i_{1,j}\iota_{j+1} + r_2\alpha_{j+1},\end{aligned} \tag{49}$$

$$\begin{aligned}h\dot\beta_j = {}& c_j(\iota_j - \beta_j) - r_2\beta_{j-1} + (i_{1,j} - i_{3,j} + i_4(\rho_j^2 + \iota_j^2))\rho_j \\ &- i_{1,j}\rho_{j+1} + (r_{1,j} + 2r_2 - r_{3,j} + r_4(\rho_j^2 + \iota_j^2))\iota_j \\ &- (r_{1,j} + 2r_2)\iota_{j+1} + r_2\beta_{j+1},\end{aligned} \tag{50}$$

for $j = 1, \ldots, N-1$. Furthermore, the two summations in (41) equal $h\dot\alpha_0$, and the two summations in (42) equal $h\dot\beta_0$. Keeping this in mind, and

inserting (49)–(50) and (41)–(42) into (48), we get

$$\begin{aligned}\dot{V} \leq & (\rho_0-\alpha_0)(-c_0(\rho_0-\alpha_0)+r_2\rho_1-r_2\alpha_1)\\ & +(\iota_0-\beta_0)(-c_0(\iota_0-\beta_0)+r_2\iota_1-r_2\beta_1)\\ & +\sum_{j=1}^{N-1}[(\rho_j-\alpha_j)(-r_2\rho_{j-1}-c_j(\rho_j-\alpha_j)\\ & +r_2\alpha_{j-1}+r_2\rho_{j+1}-r_2\alpha_{j+1})\\ & +(\iota_j-\beta_j)(-r_2\iota_{j-1}-c_j(\iota_j-\beta_j)+r_2\beta_{j-1}\\ & +r_2\iota_{j+1}-r_2\beta_{j+1})]-r_2\rho_N(\rho_{N-1}-\alpha_{N-1})\\ & -r_2\iota_N(\iota_{N-1}-\beta_{N-1})\\ & -(c_N-r_2)(\rho_N^2+\iota_N^2)-\frac{c}{2}\|(\rho,\iota)\|^2_{L_2(x_d,\infty)}.\end{aligned} \tag{51}$$

After rearranging the terms, we get

$$\begin{aligned}\dot{V} \leq & -\sum_{j=0}^{N-1}c_j\Big((\rho_j-\alpha_j)^2+(\iota_j-\beta_j)^2\Big)\\ & +r_2(\rho_0-\alpha_0)(\rho_1-\alpha_1)+r_2(\iota_0-\beta_0)(\iota_1-\beta_1)\\ & +\sum_{j=1}^{N-1}[(\rho_j-\alpha_j)(-r_2\rho_{j-1}+r_2\alpha_{j-1}+r_2\rho_{j+1}\\ & -r_2\alpha_{j+1})+(\iota_j-\beta_j)(-r_2\iota_{j-1}+r_2\beta_{j-1}+r_2\iota_{j+1}\\ & -r_2\beta_{j+1})]-r_2\rho_N(\rho_{N-1}-\alpha_{N-1})-r_2\iota_N(\iota_{N-1}\\ & -\beta_{N-1})-(c_N-r_2)(\rho_N^2+\iota_N^2)-\frac{c}{2}\|(\rho,\iota)\|^2_{L_2(x_d,\infty)}.\end{aligned} \tag{52}$$

By splitting up the summation and changing summation indices, we obtain

$$\begin{aligned}\dot{V} \leq & -\sum_{j=0}^{N-1}c_j\Big((\rho_j-\alpha_j)^2+(\iota_j-\beta_j)^2\Big)\\ & +r_2(\rho_0-\alpha_0)(\rho_1-\alpha_1)+r_2(\iota_0-\beta_0)(\iota_1-\beta_1)\\ & -r_2(\rho_1-\alpha_1)(\rho_0-\alpha_0)-r_2\sum_{j=1}^{N-2}(\rho_{j+1}-\alpha_{j+1})\\ & \times(\rho_j-\alpha_j)+r_2(\rho_{N-1}-\alpha_{N-1})(\rho_N-\alpha_N)\\ & +r_2\sum_{j=1}^{N-2}(\rho_j-\alpha_j)(\rho_{j+1}-\alpha_{j+1})\\ & -r_2(\iota_1-\beta_1)(\iota_0-\beta_0)\\ & -r_2\sum_{j=1}^{N-2}(\iota_{j+1}-\beta_{j+1})(\iota_j-\beta_j)\\ & +r_2(\iota_{N-1}-\beta_{N-1})(\iota_N-\beta_N)\\ & +r_2\sum_{j=1}^{N-2}(\iota_j-\beta_j)(\iota_{j+1}-\beta_{j+1})\\ & -r_2\rho_N(\rho_{N-1}-\alpha_{N-1})-r_2\iota_N(\iota_{N-1}-\beta_{N-1})\\ & -(c_N-r_2)(\rho_N^2+\iota_N^2)-\frac{c}{2}\|(\rho,\iota)\|^2_{L_2(x_d,\infty)},\end{aligned} \tag{53}$$

and after cancellation of terms, we have

$$\begin{aligned}\dot{V} \leq & -\sum_{j=0}^{N-1}c_j\Big((\rho_j-\alpha_j)^2+(\iota_j-\beta_j)^2\Big)\\ & -(c_N-r_2)(\rho_N^2+\iota_N^2)\\ & -\frac{c}{2}\|(\rho,\iota)\|^2_{L_2(x_d,\infty)}.\end{aligned} \tag{54}$$

In the last step we used the fact that $\alpha_N=\beta_N=0$. It now follows from standard results [9], that the equilibrium point $(\rho_0,\iota_0,\rho_1,\iota_1,\ldots,\rho_N,\iota_N)=0$ is globally asymptotically stable, and that

$$\|(\rho,\iota)\|^2_{L_2(x_d,\infty)}\to 0 \quad \text{as } t\to\infty. \tag{55}$$

Having established that $\rho_0,\iota_0,\rho_1,\iota_1\to 0$ as $t\to\infty$, it follows from (10) in Lemma 3, and its semi-discrete version (34), that

$$\|(\rho,\iota)\|^2_{L_2(-\infty,x_u)}\to 0 \quad \text{as } t\to\infty. \tag{56}$$

Remark 5. The backstepping procedure used for the control design starts at node N, which corresponds to $x=x_d$, and steps in the direction of $x=x_u$. For every step of backstepping, a new measurement upstream is clearly needed. However, the need for measurements also propagates one step downstream for each step of backstepping. Therefore, the discretization used for control design has to span an interval twice the size of the core, or more precisely, the interval $[x_u, 2x_d-x_u]$.

Remark 6. Although Theorem 4 provides a stabilizing controller for the discretized system of arbitrary order, it does not guarantee that the feedback gain stays bounded as $h\to 0$. Thus, the result does not hold in the limit of infinitely fine discretizations. In [3], a target system with known stability properties is chosen, and the control law designed such that the dynamics of the closed loop system becomes that of the target system. The target system is chosen such that the parabolic character of the system is maintained, in order to guarantee that the controller has finite gain. If the

domain were finite, an appropriate target system in the present case would be

$$\frac{\partial p}{\partial t} = -\left(a_{R_1}(x)\frac{\partial}{\partial x} + a_{R_2}\frac{\partial^2}{\partial x^2} + b_R(x)\right)p + \left(a_{I_1}(x)\frac{\partial}{\partial x} + a_{I_2}\frac{\partial^2}{\partial x^2} + a_{I_4}(x)\right)q, \quad (57)$$

$$\frac{\partial q}{\partial t} = -\left(a_{I_1}(x)\frac{\partial}{\partial x} + a_{I_2}\frac{\partial^2}{\partial x^2} + a_{I_4}(x)\right)p - \left(a_{R_1}(x)\frac{\partial}{\partial x} + a_{R_2}\frac{\partial^2}{\partial x^2} + b_R(x)\right)q, \quad (58)$$

where the function $b_R(x)$ satisfies

$$\frac{1}{4a_{R_2}}a_{I_1}^2(x) - \frac{\partial a_{R_1}}{\partial x} + b_R(x) > \frac{1}{2}c, \quad \text{for all } x, \quad (59)$$

$$b_R(x) = a_{R_4}(x), \quad \text{for } x \notin [x_d, x_u], \quad (60)$$

with $c > 0$. In view of Assumption 2, $x_u < x_d$ and c exist such that this is possible. A proof analogous to that of Lemma 3, provides asymptotic stability of the zero-solution of (57)–(58) in the L_2 norm. However, in the present case, the infinite domain in combination with the nonlinearity prevents an easy choice of target system. The price we pay is a controller without a guarantee that the gain won't grow unbounded as N tends to infinity. However, when a backstepping design is pursued with a low number of steps, motivated by a low number of unstable eigenvalues, the difference between the two approaches is small and the issue of convergence as N tends to infinity does not arise.

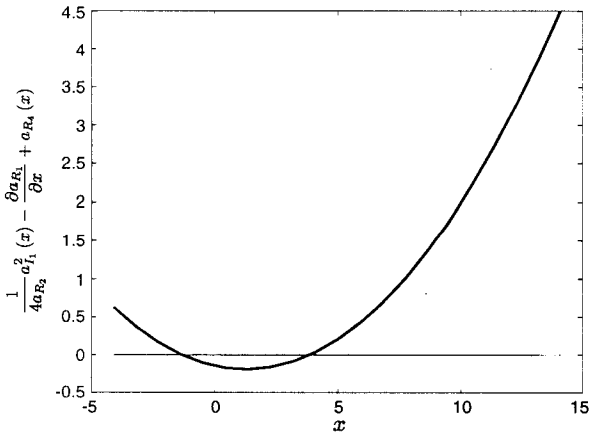

Fig. 3. Graphical determination of the constants x_u and x_d for $R = 50$ using the numerical coefficients in [12].

4. Simulation Study

In order to demonstrate the performance of our backstepping controller, we present a simulation example. We set the Reynolds number to $R = 50$, and discretize (7)–(8) on the domain $x \in [-5, 15]$ using 400 nodes. Homogeneous Dirichlet boundary conditions are enforced at $x = -5$ and $x = 15$. Next, we plot the expression (20), that is

$$\frac{1}{4a_{R_2}}a_{I_1}^2(x) - \frac{\partial a_{R_1}}{\partial x} + a_{R_4}(x), \quad (61)$$

on our chosen domain. The result is shown in Fig. 3. By inspection of the graph, we pick $x_u = -1.32$ and $x_d = 3.85$. The nodes of the discretization, along with x_u and x_d, are plotted in Fig. 4. As the figure shows, applying Theorem 4 at this point requires in the order of 100 backstepping steps. Instead, we use a discretization that is coarser for the control design, keeping only about every 40th node. The remaining nodes, which are sensors, are shown in Fig. 4 as circles. Now, only three steps of backstepping are required. The controller is generated using the symbolic toolbox in MATLAB, and is too complicated to write here. The first row of graphs in Fig. 5 shows the values of (ρ, ι) as a function of time and space for the uncontrolled case. The figure indicates spatial unsteadiness reminiscent of vortex shedding. The second row of graphs in Fig. 5 shows the controlled case. Clearly, the states in the entire domain are effectively driven to zero by the control. Figure 6 shows the performance of the controller in terms of the output (ρ, ι) from one of the sensors (identified in Fig. 4). As the figure shows, the system is in the state of natural shedding for a couple of cycles, and then, at $t = 50$, the control is turned on driving the state to

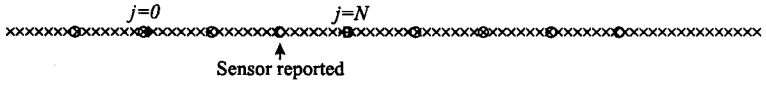

Fig. 4. Locations of every fifth grid point (×), sensors (◦), and $[x_u, x_d]$ (+). Only about every fortieth node is used for feedback, requiring three steps of backstepping in this case.

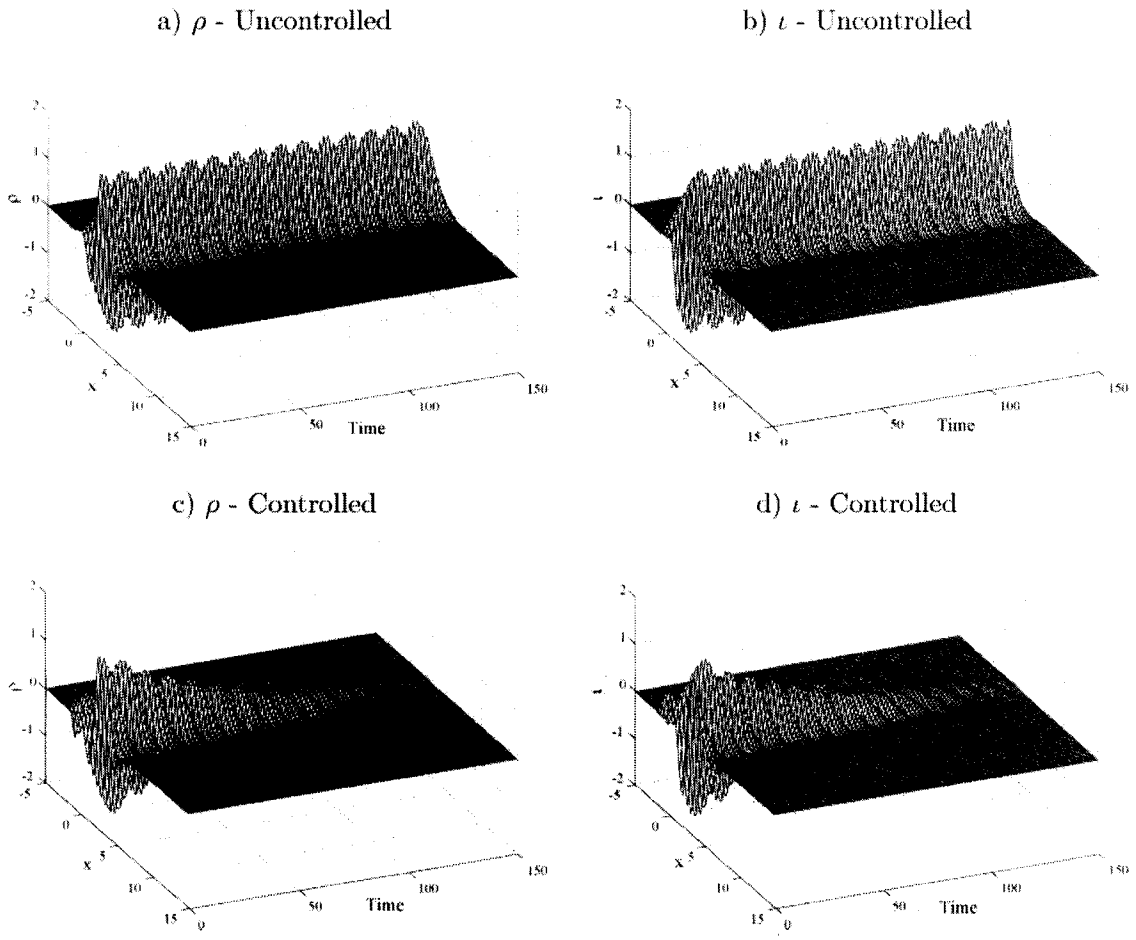

Fig. 5. Comparison of the uncontrolled and controlled cases.

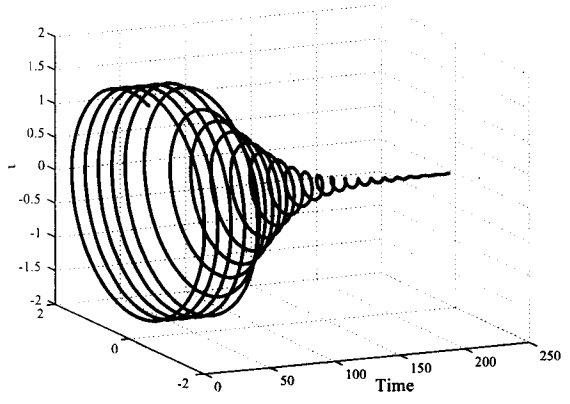

Fig. 6. Time evolution of (ρ, ι) at sensor location number 4. Feedback is turned on at $t = 150$.

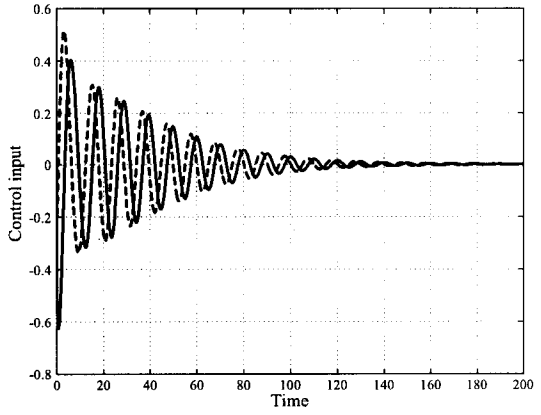

Fig. 7. Real (solid) and imaginary (dashed) parts of the control input.

zero. Figure 7 shows the corresponding control effort.

Remark 7. The quadratic form of (61) ensures the existence of a minimal interval (x_1, x_2) (or possibly empty), in which (61) is negative. For the stability results to hold, x_u and x_d must be chosen such that $(x_1, x_2) \subset [x_u, x_d]$. So, there are infinitely many valid choices for x_u and x_d, but a case can be made for

choosing the interval $[x_u, x_d]$ as small as possible. First, for a given spatial resolution for the control design, fewer backstepping steps will be needed, resulting in a simpler control law. Second, by pushing the point of actuation (x_u) far upstream, its effect on the region of instability, which is given by the minimal interval (x_1, x_2), will diminish due to the increasingly stronger local dissipativity of the system when moving away from the core.

5. Conclusions

We have shown that global asymptotic stabilization of a nonlinear Ginzburg–Landau model of vortex shedding from bluff bodies can be achieved using backstepping. Stabilization was achieved for finite difference discretizations of arbitrary order of the core flow. The infinite domain in combination with the nonlinearity prevents an easy choice of target system in the sense of [3]. The consequence is a controller for which finite gain is not guaranteed, and stabilization in the limit of inifinitely fine discretization does therefore not follow from the results. The question of convergence under infinitely fine discretizations is very important and very difficult. For nonlinear PDEs under backstepping type feedback laws no results exist proving convergence for arbitrarily large initial data. Recent results in [6] prove convergence in the linear case. However, when a backstepping design is pursued with a low number of steps, motivated by a low number of unstable eigenvalues, the difference between the two approaches is small and the issue of convergence in the limit of infinitely fine discretization does not arise. The potential of using low order discretizations for the control design was demonstrated in simulations. This feature is also important from a controller complexity point of view, since the nonlinearity of the system causes the complexity of the controller to increase very rapidly with increasing number of backstepping steps. Future research directions include dealing with the convergence issue, and the output feedback problem.

Acknowledgements

We thank Peter A. Monkewitz and Eric Lauga for their help determining the numerical coefficients used in the simulations. This work was supported by the Office of Naval Research, the Air Force Office of Scientific Research, the National Science Foundation, and the Norwegian Research Council.

References

1. Aamo OM, Krstić M. Feedback control of particle dispersion in bluff body wakes (submitted)
2. Armaou A, Christofides PD. Wave suppression by nonlinear finite-dimensional control. Chem Eng Sci 2000; 55: 2627–2640
3. Bošković DM, Krstić M. Nonlinear stabilization of a thermal convection loop by state feedback. Automatica 2001; 37(12): 2033–2040
4. Bošković DM, Krstić M. Stabilization of a solid propellant rocket instability. Proceedings of the 40th IEEE conference on decision and control. Orlando, Florida, USA, 2002
5. Bošković DM, Krstić M. Backstepping control of chemical tubular reactors. Comp Chem Eng 2002; 26(7–8): 1077–1085
6. Bošković DM, Balogh A, Krstić M. Backstepping in infinite dimension for a class of parabolic distributed parameter systems. Math Control, Signals, Syst 2003; 16: 44–75
7. Gunzburger MD, Lee HC, Feedback control of Karman vortex shedding. Trans ASME 1996; 63: 828–8350
8. Huerre P, Monkewitz PA. Local and global instabilities in spatially developing flows. Annu Rev Fluid Mech 1990; 22: 473–537
9. Krstić M, Kanellakopoulos I, Kokotović P. Nonlinear and adaptive control design. John Wiley & Sons, Inc., 1995
10. Lauga E, Bewley TR. H_∞ control of linear global instability in models of non-parallel wakes. Proceedings of the second international symposium on turbulence and shear flow phenomena. Stockholm, Sweden, 2001
11. Park DS, Ladd DM, Hendricks EW. Feedback control of von Kármán vortex shedding behind a circular cylinder at low Reynolds numbers. Phys Fluids 1994; 6(7): 2390–2405
12. Roussopoulos K, Monkewitz PA. Nonlinear modelling of vortex shedding control in cylinder wakes. Phys D 1996; 97: 264–273
13. Temam R. Infinite-dimensional dynamical systems in mechanics and physics, 2nd ed. Springer, 1997
14. Williamson CHK. Vortex dynamics in the cylinder wake. Annu Rev Fluid Mech 1996; 28: 477–539

Appendix A. Coefficients for the Ginzburg–Landau Equation

The numerical coefficients below are taken from [12, Appendix A]:

$$R_c = 47, \tag{62}$$

$$x^t = 1.183 - 0.031\mathrm{i}, \tag{63}$$

$$\omega_0^t = 0.690 + 0.080\mathrm{i} + (-0.00159 + 0.00447\mathrm{i})(R - R_c), \tag{64}$$

$$k_0^t = 1.452 - 0.844\mathrm{i} + (0.00341 + 0.011\mathrm{i})(R - R_c), \tag{65}$$

$$\omega_{kk}^t = -0.292\mathrm{i}, \tag{66}$$

$$\omega^t_{xx} = 0.108 - 0.057\mathrm{i}, \tag{67}$$
$$k^t_x = 0.164 - 0.006\mathrm{i}, \tag{68}$$
$$\omega_0(x) = \omega^t_0 + \tfrac{1}{2}\omega^t_{xx}(x - x^t)^2, \tag{69}$$
$$k_0(x) = k^t_0 + k^t_x(x - x^t), \tag{70}$$
$$a_1(x) = -\omega^t_{kk}k_0(x), \tag{71}$$
$$a_2 = -\tfrac{1}{2}\mathrm{i}\omega^t_{kk}, \tag{72}$$
$$a_3 = -0.638 + 0.191\mathrm{i} + (0.0132 - 0.00399\mathrm{i})(R - R_c), \tag{73}$$
$$a_4(x) = (\omega_0 + \tfrac{1}{2}\omega^t_{kk}k_0^2(x))\mathrm{i}, \tag{74}$$
$$a_5 = -0.0225 + 0.0671\mathrm{i}. \tag{75}$$

Based on these parameters, we obtain

$$a_{R_1}(x) = 0.24289 - 0.003212(R - R_c) + 1.752 \times 10^{-3}x, \tag{76}$$
$$a_{I_1}(x) = 0.36739 + 0.00099572(R - R_c) + 4.7888 \times 10^{-2}x, \tag{77}$$
$$a_{R_2} = -0.146, \tag{78}$$
$$a_{I_2} = 0, \tag{79}$$
$$a_{R_3} = -0.638 + 0.0132(R - R_c), \tag{80}$$
$$a_{I_3} = 0.191 - 0.00399(R - R_c), \tag{81}$$
$$a_{R_4}(x) = 9.3917 \times 10^{-2} - 5.4541 \times 10^{-4}(R - R_c) - 1.5968 \times 10^{-5}(R - R_c)^2 - 1.1985 \times 10^{-2}x, + 1.8257 \times 10^{-4}(R - R_c)x + 3.2422 \times 10^{-2}x^2, \tag{82}$$
$$a_{I_4}(x) = 0.45783 + 1.6230 \times 10^{-3}(R - R_c)1.0953 \times 10^{-5}(R - R_c)^2 - 0.16804x + 5.2079 \times 10^{-4}(R - R_c)x + 5.3713 \times 10^{-2}x^2, \tag{83}$$
$$a_{R_5} = -0.0255, \tag{84}$$
$$a_{I_5} = 0.0671. \tag{85}$$